

Non-resonant energy harvesting via an adaptive bistable potential

This content has been downloaded from IOPscience. Please scroll down to see the full text.

2016 Smart Mater. Struct. 25 015010

(<http://iopscience.iop.org/0964-1726/25/1/015010>)

View [the table of contents for this issue](#), or go to the [journal homepage](#) for more

Download details:

IP Address: 18.9.61.112

This content was downloaded on 15/07/2017 at 20:06

Please note that [terms and conditions apply](#).

You may also be interested in:

[A review of the recent research on vibration energy harvesting via bistable systems](#)

R L Harne and K W Wang

[Nonlinear M-shaped broadband piezoelectric energy harvester for very low base accelerations: primary and secondary resonances](#)

S Leadenham and A Erturk

[Finite element modeling of nonlinear piezoelectric energy harvesters with magnetic interaction](#)

Deepesh Upadrashta and Yaowen Yang

[A broadband electromagnetic energy harvester with a coupled bistable structure](#)

D Zhu and S P Beeby

[Novel piezoelectric bistable oscillator architecture for wideband vibration energy harvesting](#)

W Q Liu, A Badel, F Formosa et al.

[Energy harvesting from human motion: an evaluation of current nonlinear energy harvesting solutions](#)

P L Green, E Papatheou and N D Sims

[Bistable energy harvesting enhancement with an auxiliary linear oscillator](#)

R L Harne, M Thota and K W Wang

[Modeling and experimental verification of doubly nonlinear magnet-coupled piezoelectric energy harvesting from ambient vibration](#)

Shengxi Zhou, Junyi Cao, Wei Wang et al.

[Dynamics and coherence resonance of tri-stable energy harvesting system](#)

Li Haitao, Qin Weiyang, Lan Chunbo et al.

Non-resonant energy harvesting via an adaptive bistable potential

Ashkan Haji Hosseinloo and Konstantin Turitsyn

Massachusetts Institute of Technology, 77 Massachusetts Avenue, Cambridge, MA, USA

E-mail: ashkanhh@mit.edu and turitsyn@mit.edu

Received 25 May 2015, revised 14 October 2015

Accepted for publication 29 October 2015

Published 23 November 2015



CrossMark

Abstract

Narrow bandwidth and easy detuning, inefficiency in broadband and non-stationary excitations, and difficulties in matching a linear harvester's resonance frequency to low-frequency excitations at small scales, have convinced researchers to investigate nonlinear, and in particular bistable, energy harvesters in recent years. However, bistable harvesters suffer from co-existing low and high energy orbits, and sensitivity to initial conditions, and have recently been proven inefficient when subjected to many real-world random and non-stationary excitations. Here, we propose a novel non-resonant buy-low-sell-high strategy that can significantly improve the harvester's effectiveness at low frequencies in a much more robust fashion. This strategy could be realized by a passive adaptive bistable system. Simulation results confirm the high effectiveness of the adaptive bistable system following a buy-low-sell-high logic when subjected to harmonic and random non-stationary walking excitations compared to its conventional bistable and linear counterparts.

Keywords: energy harvesting, bistable potential, adaptive, buy-low-sell-high strategy, piezoelectric, non-resonant

(Some figures may appear in colour only in the online journal)

1. Introduction

The short life span, miniaturization and scalability difficulties, replacement and maintenance issues, and relatively very low pace of energy density improvement of conventional batteries [1, 2] have convinced many researchers and scientists to consider energy harvesters as potential replacements for batteries in many applications. In particular, vibratory energy harvesters have captured enormous attention in the last decade due to the universality and abundant availability of vibratory energy sources.

Linear harvesters exploiting resonance phenomena suffer from the narrow bandwidth of efficient harvesting. The narrow resonance bandwidth renders linear harvesters very inefficient when subjected to non-stationary excitation where excitation characteristics, e.g. dominant frequency, change over time, or when the harvester is exposed to broadband random vibration where the excitation power is spread over a wide frequency range. Non-stationary and random vibration are in fact more common than harmonic excitation in many practical applications [3–6]. To overcome this issue different

techniques such as resonance tuning, multi-modal energy harvesting, frequency up-conversion, and more recently purposeful inclusion of nonlinearity have been suggested [7, 8]. Among these techniques, deliberate introduction of nonlinearity, particularly bistable nonlinearity, has been the focus of the research in vibration energy harvesting since 2009. However, recent studies have revealed that monostable and bistable nonlinear harvesters do not always outperform their linear counterparts.

One of the main issues with bistable harvesters when subjected to harmonic excitation is the non-uniqueness of the solution, with co-existing low-energy and high-energy orbits at a given excitation frequency and amplitude [9–12]. In fact, for a monostable nonlinear harvester the probability of converging to the low-energy orbit is higher than that of the high-energy orbit [13]. Also, Masana and Daqaq [14] showed that for a given excitation level, a bistable harvester's performance is very sensitive to the potential shape (shallow versus deep wells).

The performance of the bistable harvester is further diminished when it is subjected to random excitation. Daqaq [15] showed that for an inductive energy harvester with

negligible inductance, bistability (and in general any stiffness nonlinearity) does not provide any improvement over a linear harvester when excited by white noise. Cottone *et al* [16] and Daqaq [17] showed that when driven by white noise, a necessary condition for the bistable harvester to outperform its linear counterpart is to have a small ratio of mechanical to electrical time constants. They along with other researchers [18–20] showed that for a given noise intensity, the output power is highly dependent on the shape of the bistable potential. Zhao and Erturk [20] showed that the bistable harvester could outperform its linear counterpart only in a narrow region where noise intensity is slightly above the threshold of interwell oscillations.

The bistable harvester becomes even less efficient and less robust when it is excited by more realistic and real-world random vibrations (not white noise). Using real vibration measurements (of human walking motion and bridge vibration) in simulations of idealized energy harvesters, Green *et al* [21] showed that, although the benefits of deliberately inducing dynamic nonlinearities into such devices have been shown for the case of Gaussian white noise excitations, the same benefits could not be realized for real excitation conditions.

In this paper, we propose a non-resonant adaptive bistable harvester that is more robust to changes in input excitation parameters and that works more effectively under both harmonic and random excitations than its conventional linear and bistable counterparts. In the proposed harvester, the potential barrier changes adaptively following a buy-low-sell-high strategy [22].

2. Adaptive bistable harvester

In this study, we consider both capacitive and inductive harvesters (with a single degree of freedom in the mechanical domain) with an adaptive bistable potential. Here, the adaptive bistable potential refers to a potential whose shape, in particular the barrier height, could change according to a logic in an adaptive fashion. Adaptive bistability could be realized in different ways that will briefly be discussed later in the paper. But first we need to find the logic according to which the bistability changes adaptively.

The idea of finding a strategy to maximize the harvested energy was first introduced in seminal works by Mitcheson [23, 24] as a Coulomb force parametric generator and Ramlan [25] for harmonic excitation. Heit and Roundy [26] also investigated the optimal harvesting force and displacement trajectory for single and multiple sinusoid input in the absence of displacement limits. In a more advanced fashion, Halvorsen *et al* [27] treated both arbitrary general waveforms in the absence of displacement limits and periodic waveforms with displacement limits. More recently, the authors developed a strategy to maximize the harvested energy for general arbitrary waveforms and an ideal harvester in the presence of displacement limits [22]. For the sake of readability and its application to the bistable system, its key concepts are discussed next.

2.1. Adaptive bistability logic: buy-low-sell-high

To find the logic, we consider a model of a single-degree-of-freedom ideal energy harvester characterized by the mass m and displacement $x(t)$ that is subject to the energy harvesting force $f(t)$ and exogenous excitation force $F(t)$. Then, the equation of motion will simply be

$$m\ddot{x}(t) = F(t) + f(t). \quad (1)$$

Here we assume that the ideal harvesting force can harvest all the energy that flows to the system (there is no long-term accumulation of energy in the system). Hence, maximizing the harvested energy will be equivalent to maximizing the energy flow to the system. In other words, we want to maximize

$$E_{\max} = \max_{x(t)} \int dt F(t)\dot{x}(t) \quad (2)$$

over admissible trajectories of $x(t)$. It is easy to show that this integral is unbounded if $x(t)$ is unconstrained. Indeed, the trajectory defined by a simple relation $\dot{x}(t) = \lambda F(t)$ that can be realized with the harvesting force $f = m\lambda\dot{F} - F$ results in a harvesting rate of λF^2 , which can be made arbitrarily large by increasing the mobility constant λ . This trivial observation illustrates that the question of fundamental limits is only well-posed for models that incorporate some technological or physical constraints. This is a general observation that applies to most of the known fundamental limits. For example, the Carnot cycle limits the efficiency of cycles with bounded working fluid temperature, and Shannon capacity defines the limits for signals with bounded amplitudes and bandwidth.

As a common constraint to vibratory energy harvesters, we constrain the harvester displacement in a symmetric fashion i.e. $|x(t)| \leq x_{\max}$, where x_{\max} is the displacement limit. Rewriting equation (2) as $-\int dt \dot{F}(t)x(t)$, it can be seen by inspection that the integral is maximized by the optimal trajectory:

$$x_*(t) = -x_{\max} \text{sign}[\dot{F}(t)]. \quad (3)$$

This optimal trajectory is indeed realizable by the ideal harvesting force of $f(t) = m\ddot{x}_*(t) - F(t)$. The interpretation of equation (3) is easy; it says that when $F(t)$ is increasing, $x(t)$ should be kept at its lower limit, and vice versa, when $F(t)$ is decreasing, $x(t)$ should be kept at its upper limit. Thus, the transitions between displacement limits occur when the sign of $\dot{F}(t)$ is changing, i.e. at the extrema of $F(t)$. In other words, in this logic, the harvester mass is kept at its lowest position ($-x_{\max}$) until the excitation force $F(t)$ reaches its maximum, when the mass should be pushed to its highest position (x_{\max}) (either by the excitation force, or by the harvesting force if the local maximum of the excitation force is still negative or not big enough to push the mass to the highest position limit¹). Similar dynamics occur in the reverse direction, and this

¹ It should be noted that, even though the harvesting force is injecting energy into the system in this case during a short period, the net amount of harvested energy will be positive at the end. This is because the injection of energy by the harvesting force will pay off when the next excitation force minimum is reached.

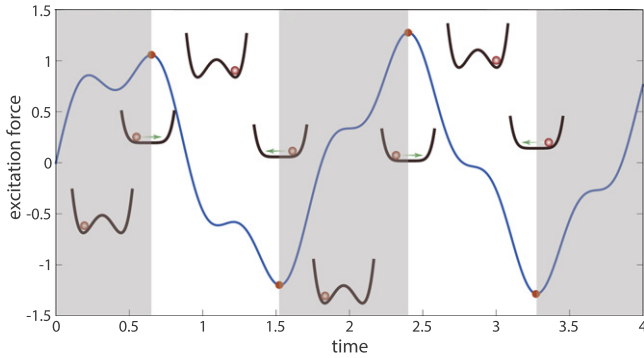


Figure 1. Passive BLSH strategy realized by an adaptive bistable potential for an arbitrary excitation input. The transition from one displacement limit to the other is highlighted by the change in the background color.

strategy continues in the same fashion at every extremum of the excitation force $F(t)$.

If the harvester is incapable of injecting energy into the system (a passive-only harvester), the harvested mass should traverse between the limits ($\pm x_{\max}$) by the excitation force $F(t)$ only. In this case, the logic is slightly modified; the harvester mass should be kept at its lowest (highest) displacement limit until the largest maximum (most-negative minimum) of the excitation force is reached. Only then is the harvester mass pushed from one displacement limit to the other. This logic is very similar to the well-known buy-low-sell-high strategy in the stock market; hence, we call this logic a buy-low-sell-high (BLSH) strategy hereafter.

Now the question is how to implement this logic. The BLSH strategy could be realized by an adaptive bistable potential. In essence, the passive BLSH strategy keeps the harvester mass at one end ($\pm x_{\max}$) before letting it go to the other end according to its logic. A bistable potential with stable points at $\pm x_{\max}$ and an adaptive potential barrier could do this. To realize the BLSH logic, the potential barrier should be large enough to confine the harvester mass in one well (x_{\max} or $-x_{\max}$). Then, when, according to the logic, the harvester mass should traverse to the other end, the potential barrier should vanish. This logic is schematically shown in figure 1. Note that a harvester equipped with this nonlinear logic is essentially a non-resonant harvester.

2.2. Mathematical modeling

The harvester is modeled as a lumped-parameter mechanical oscillator coupled to a simple electrical circuit via an electromechanical coupling mechanism. The formulation here is generic and could be applied to both capacitive (e.g. piezoelectric) and inductive (e.g. electromagnetic) transduction mechanisms. The nondimensionalized governing dynamic equations could be written as [8]

$$\begin{aligned} \ddot{x} + 2\zeta\dot{x} + \frac{\partial U(x, t)}{\partial x} + \kappa^2 y &= -\ddot{x}_b \\ \dot{y} + \alpha y &= \dot{x}. \end{aligned} \quad (4)$$

In the above equations, x is the oscillator's displacement relative to base displacement (x_b). Linear mechanical damping is characterized by the damping ratio ζ , and κ denotes the linear electromechanical coupling coefficient. y represents the electric quantity that would be voltage or current in capacitive or inductive transduction mechanisms, respectively, and α is the ratio of the mechanical to the electrical time constants. The adaptive bistable potential is denoted by $U(x, t)$, and the overdot denotes differentiation with respect to dimensionless time. All parameters and variables are dimensionless.

Two common techniques to realize bistability are the buckling phenomenon and magnets (to create negative stiffness) in addition to the positive mechanical stiffness. When using a magnetic field to realize bistability, if permanent magnets are replaced by electromagnets [28] (giving a controllable magnetic field) one can change the potential shape and, hence, create an adaptive bistability. A passive bistable potential admits a quartic form [29], and when made adaptive, we model it as

$$\begin{aligned} U(x, t) &= \frac{1}{2} \left(1 + \sigma(x, F, \dot{F}) r_k \right) x^2 \\ &\quad - \frac{1}{4} \sigma(x, F, \dot{F}) (1 + r_k) \frac{x^4}{x_s^2}, \end{aligned} \quad (5)$$

where $r_k < -1$ is the strength of the negative stiffness of the magnetic field relative to the linear mechanical one. x_s denotes the dimensionless stable position of the bistable potential, and $\sigma(x, F, \dot{F})$ is a signal function which repeatedly switches between 1 and 0 according to the BLSH logic. The signal function depends on the system states and excitation statistics. $\sigma(x, F, \dot{F})$ is always equal to unity except when we want the harvester mass to traverse from one end to the other (according to the BLSH strategy), when it is set to zero. Based on the BLSH logic, $\sigma(x, F, \dot{F})$ could be formulated as follows

$$\sigma(x, F, \dot{F}) = \begin{cases} 0; & \dot{F}(t) = 0 \text{ and } F(t)x(t) < 0 \\ 1; & |x(t)| \approx x_{\max} \text{ and } F(t)x(t) > 0. \end{cases} \quad (6)$$

In equation (6), the signal function is set to unity when $|x(t)|$ is *approximately* and not exactly equal to x_{\max} . The reason is twofold: first, once the potential is activated the mass still oscillates in that well even though by a small amount; hence, to make sure it does not exceed the displacement limits, the potential is activated slightly before it reaches $\pm x_{\max}$. Second, once the mass reaches one well, we want to keep it trapped in that well until the condition for the release of the mass arises, i.e. the first condition in equation (6). However, before this condition has arisen, the mass oscillates slightly in that well, so its displacement will be approximately and not exactly equal to $\pm x_{\max}$. In simple words, the second condition in equation (6) says that the mass should be trapped and kept at one end once it reaches the displacement limits before the first condition arises and it is released. It is also worth mentioning that, in the limit where the potential barrier height goes to infinity, the approximation changes to equality.

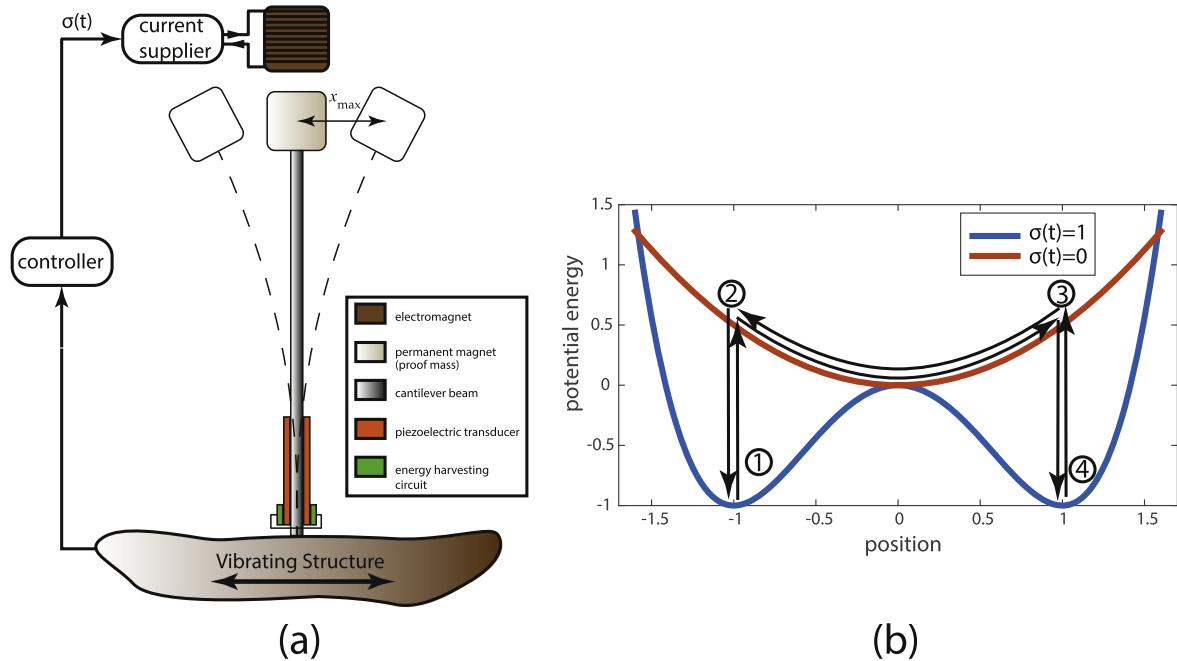


Figure 2. Energy harvesting with adaptive bistability. (a) Schematics of a cantilever energy harvester with a piezoelectric transduction mechanism equipped with adaptive bistability and (b) change in the harvester's potential function to realize the BLSH logic and the sequence of the harvester mass trajectory on admissible potential curves following the logic.

Figure 2(a) depicts an energy harvester with a piezoelectric (capacitive) transduction mechanism equipped with adaptive bistable potential. The adaptive bistability is realized by an electromagnet and a permanent magnet (the proof mass). An on/off controller is used to implement the BLSH logic. The controller senses the excitation and the harvester states and then according to the BLSH strategy sends a signal to the current supplier to supply an appropriate current ($\sigma(t) = 1$) or to shut down the current supply ($\sigma(t) = 0$).

It should be noted that using electro- and permanent magnets is not the only way to realize adaptive bistability. Although this technique is easy to implement, care should be taken to design the electromagnets with minimal losses. Since the harvester mass is at the displacement limits for a substantial fraction of the time, ohmic losses could be larger than the harvested energy if the electromagnets are poorly designed. Another possible way to realize adaptive bistability, as mentioned earlier, is via adaptive buckling. Buckling as a means to create bistability in the context of energy harvesting is well studied (see e.g. [30]). Making it adaptive could solve the issue of ohmic losses although it entails its own practical difficulties, e.g. adaptively changing the axial force to switch between the buckled and normal states of the beam.

Figure 2(b) shows how the potential shape changes based on the controller signal $\sigma(t)$, and graphically depicts the sequence of the harvester mass trajectory following BLSH logic on admissible potential curves². It should be noted with this type of implementation (equation (5) and figure 2(a)) the

² In fact when the magnetic potential is added to the system, the whole bistable potential curve should be shifted above the quadratic mechanical potential curve. This does not show up here as we have dropped a constant term in equation (5). However, this does not affect the dynamics of the system.

adaptive bistable system following BLSH logic will not always be passive. For instance, when the harvester mass is moved ① → ② (④ → ③) a positive amount of energy is added to the system because of the way the potential shape is changed. However, in the transition right before the one that adds energy, i.e. in ② → ① (③ → ④), the same amount of energy is taken out of the system; hence, the net energy injected into the system by this type of implementation is zero in half a cycle (if not at all times) when the cycle is referred to transitions from $-x_{max}$ to $+x_{max}$ and then back to $-x_{max}$. In order to have a passive system at all times, one should come up with a bistable mechanism whose potential barrier could be deepened without changing the potential energy level of its stable points, like a latching mechanism. This is not the case with the current techniques for realizing bistability (buckling and magnetic fields).

3. Results and discussion

In this section, simulation results with harmonic and experimental random excitations for a non-resonant adaptive bistable harvester are presented and compared with linear and conventional bistable harvesters. For a fair comparison, all harvesters are subjected to the same displacement limits. To this end, we first optimize the bistable system with respect to its potential shape for a given excitation input. Then the maximum displacement of the optimum bistable harvester is set as the maximum displacement limit for the linear and adaptive bistable systems. This approach greatly favors the conventional bistable system when it comes to comparison.

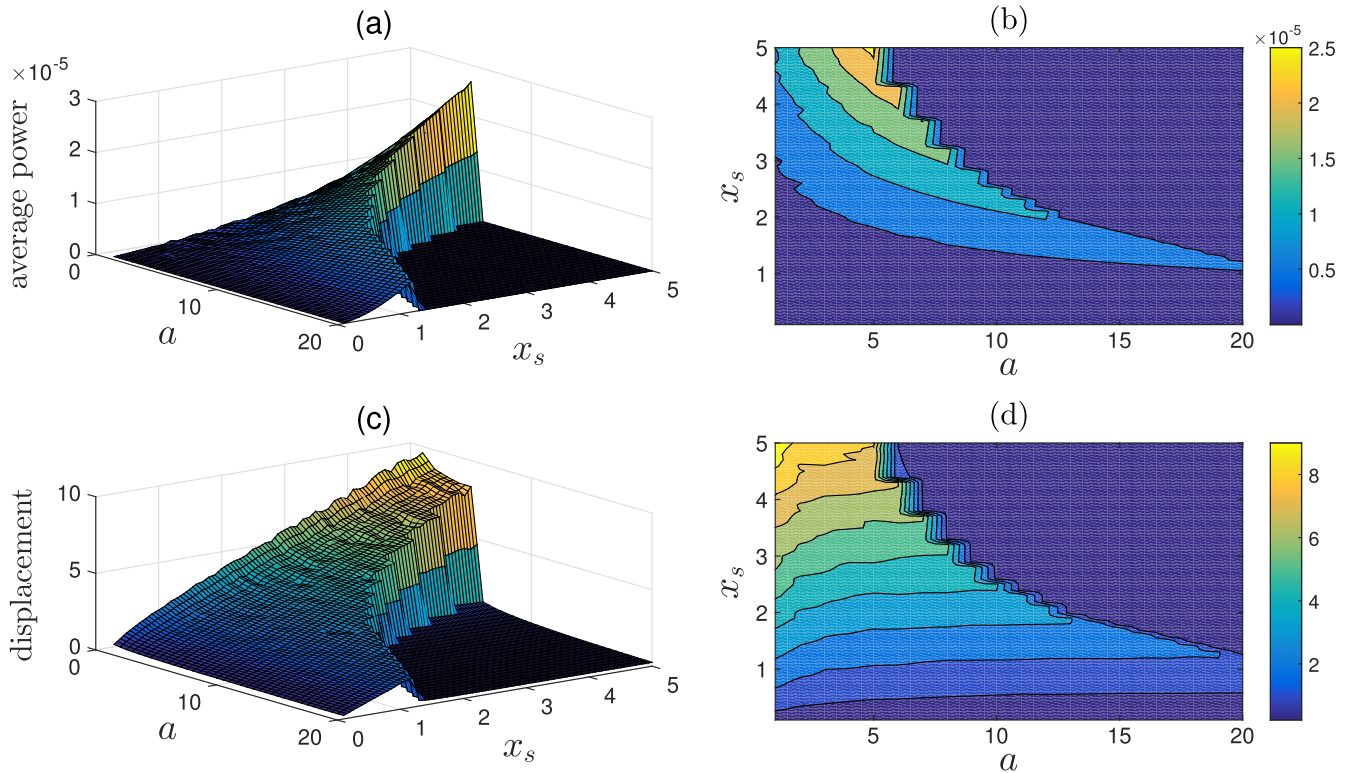


Figure 3. Energy harvesting with a conventional bistable system. (a) and (b) Surface and contour plots of average harvested power in terms of system parameters a and x_s . (c) and (d) Surface and contour plots of harvester displacement amplitude in terms of system parameters a and x_s . The other parameters are set as $F_0 = 10$, $\omega = 0.05$, $\zeta = 0.01$, $\kappa = 5$, and $\alpha = 1000$.

3.1. Harmonic excitation

The potential function considered here for the bistable system is the same as the one used for the adaptive bistable harvester with a small change in the parameter notation ($1 + r_k \rightarrow -a$). The potential used is of the form $U(x) = -\frac{1}{2}ax^2 + \frac{1}{4}a\frac{x^4}{x_s^2}$ where $a > 0$. Figure 3 shows the average power and displacement amplitude of the bistable system when subjected to harmonic excitation of the form $-\ddot{x}_b = F_0 \sin(\omega t)$. This paper intends to mainly cover the low-frequency excitation where the linear harvesters fail to work efficiently; hence, the dimensionless excitation frequency is set to $\omega = 0.05$. The average power is calculated by $\frac{1}{T} \int_0^T y^2(t) dt$ for a long simulation time T . One should note that this expression gives the normalized dimensionless average power. The dimensional instantaneous power is equal to $(m\omega_n^3 l_c^2) \alpha \kappa^2 y^2$ where m , ω_n , and l_c are the harvester mass, time-scaling frequency, and length scale, respectively. Hence, the average power used here is nondimensionalized by $m\omega_n^3 l_c^2$, and further normalized by $\alpha \kappa^2$.³

It can be seen from figure 3 that the average power increases monotonically with a and x_s up to a maximum and then drops sharply. This is where the interwell oscillation turns into intrawell oscillation (the potential barrier increases linearly with a and x_s^2). A drastic decrease in the amplitude

³ Since we are not optimizing the power with respect to α and κ it is fine to normalize the power by $\alpha \kappa^2$.

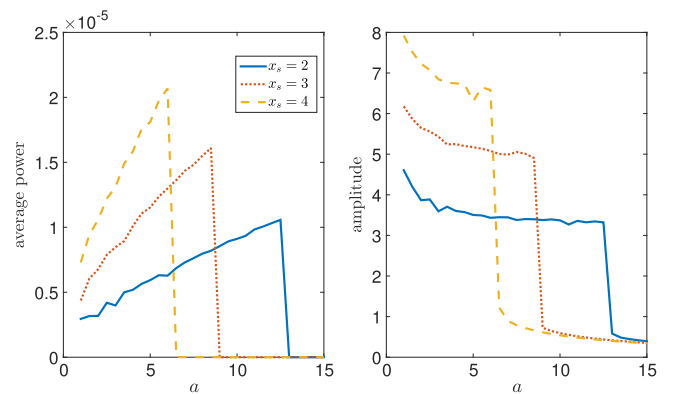


Figure 4. Average harvested power (on the left) and harvester displacement amplitude (on the right) of the conventional bistable energy harvester as a function of the potential parameter a for three different values of the parameter $x_s = 2, 3, 4$. The other simulation parameters are the same as those in figure 3.

of the oscillations verifies this. It should be noted that for values below the optimum value of a (for a given x_s), the system is still in interwell motion; however, the power monotonically decreases as a is decreased from its optimum value. This can be seen more clearly in figure 4. This suggests the robustness issues with the conventional bistable system, that is, the harvester works efficiently only when the potential barrier is slightly below its critical value, when it triggers the interwell oscillations, which agrees with Zhao and Etrurk's claim [20].

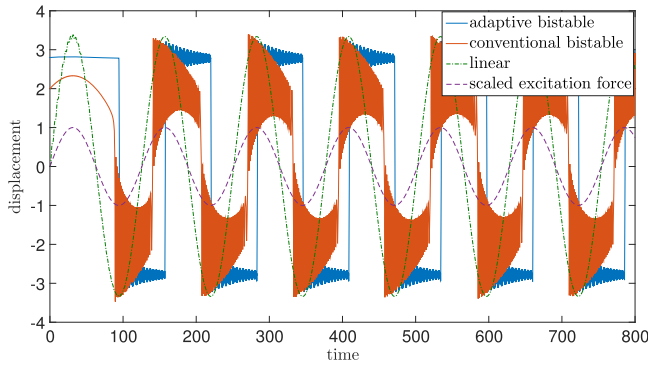


Figure 5. Displacement time histories of linear, conventional bistable, and adaptive bistable energy harvesters subjected to harmonic excitation with excitation amplitude $F_0 = 10$, and frequency $\omega = 0.05$. The other simulation parameters are $\zeta = 0.01$, $\kappa = 5$, and $\alpha = 1000$.

Next, we compare the performance of the adaptive bistable harvester with that of optimized conventional bistable and linear harvesters when they are subjected to harmonic excitation. To this end, we first optimize the parameters of the bistable system for given excitation inputs and displacement limits. The same harmonic excitation used in figures 3 and 4 is considered here ($F_0 = 10$ and $\omega = 0.05$). According to figures 3 and 4 the optimal parameters corresponding to maximum displacement of 3.4 are $x_s = 2$ and $a = 12$. For a fair comparison, the parameters of the adaptive bistable and linear harvesters are set such that their maximum displacements do not exceed this value ($r_k = -300$ and $x_s = 2.8$ for the adaptive bistable harvester and the natural frequency of $\sqrt{3}$ for the linear harvester).

Figures 5 and 6 show time histories of the displacement and electrical domain state (voltage or current for capacitive or inductive transduction mechanisms, respectively) for the three adaptive bistable, conventional bistable, and linear harvesters. According to the figures, although they all have the same maximum displacement, the maximum induced voltage (current) in them is quite different with the adaptive bistable harvester having the largest and the linear having the smallest induced voltage (current). One could notice the BLSH logic in the adaptive bistable harvester by comparing the moments of the transition from one end to the other and the excitation force extrema. It should also be noted that the conventional bistable harvester is trying to mimic the BLSH strategy in a less effective way.

Another way to compare the harvesters' performances is via their phase portraits. Figure 7(a) shows these phase portraits. As seen in the figure, the transition of the oscillator's mass between the two displacement limits occurs at a higher velocity for the adaptive bistable harvester than for the other two. The force–displacement diagram in figure 7(b) illustrates even better how the adaptive bistable harvester outperforms the other two. This diagram shows the force capable of doing positive work versus displacement. An ideal harvester, i.e. a harvester with BLSH strategy and ideal harvesting force, will have a perfect rectangle on this diagram, given the displacement limits. This rectangle represents the maximum amount

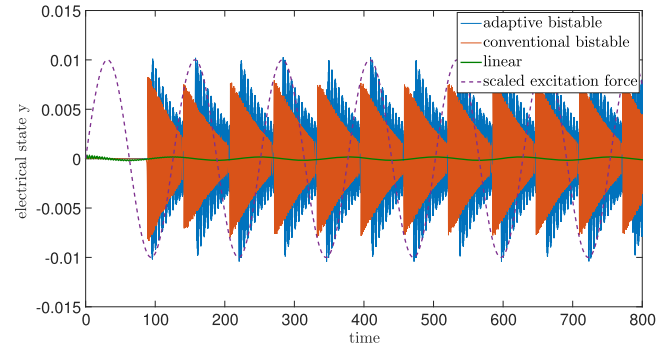


Figure 6. Electrical state (voltage or current depending on transduction mechanism) time histories of linear, conventional bistable, and adaptive bistable energy harvesters subjected to harmonic excitation with excitation amplitude $F_0 = 10$ and frequency $\omega = 0.05$. The other simulation parameters are $\zeta = 0.01$, $\kappa = 5$, and $\alpha = 1000$.

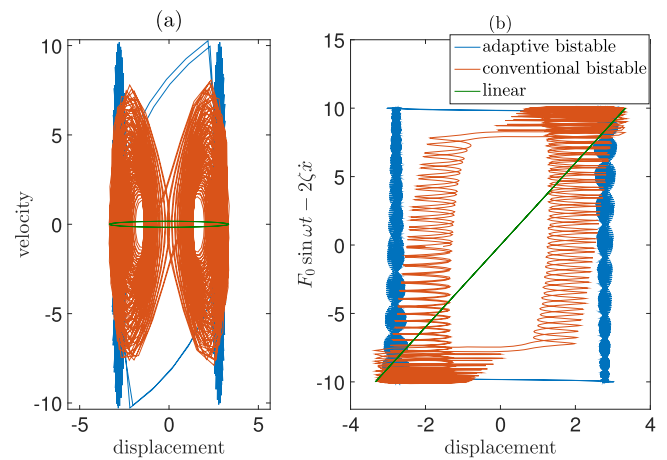


Figure 7. Phase portrait (a) and force–displacement diagram (b) of the three harvesters when subjected to harmonic excitation with excitation amplitude $F_0 = 10$ and frequency $\omega = 0.05$. The other simulation parameters are $\zeta = 0.01$, $\kappa = 5$, and $\alpha = 1000$.

of energy that could be pumped into the harvester (which will consequently be harvested by the ideal harvesting force) in one cycle. The ideal harvester with the perfect rectangle in the force–displacement diagram is analogous to the Carnot cycle with its perfect rectangle in the temperature–entropy diagram given the temperature limits of the hot and cold reservoirs. In both cases, all the other systems (harvesters and heat engines) fall within this perfect rectangle, enclosing a smaller area. Time histories of the harvested energy via the three harvesters depicted in figure 8 prove the greater effectiveness of the adaptive bistable system compared to the other two.

3.2. Random excitation: walking motion

As mentioned earlier, most real-world excitations are random and non-stationary rather than harmonic, and the linear and bistable harvesters do not work effectively when subjected to these types of excitations. To examine and compare the performance of the three harvesters with random excitations, we subject all the harvesters to experimental and relatively low-frequency walking motion. This data is experimentally

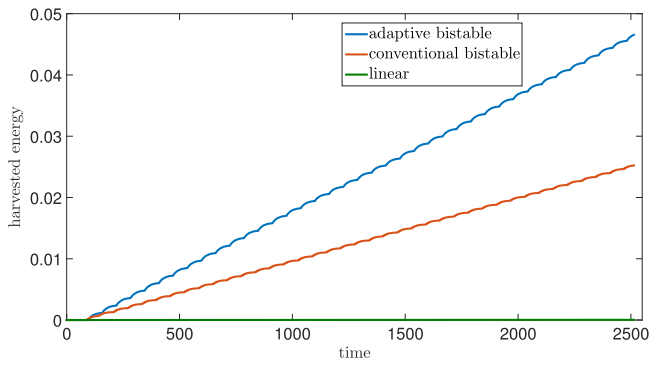


Figure 8. Time history of the energy harvested by the three harvesters when they are subjected to harmonic excitation with excitation amplitude $F_0 = 10$ and frequency $\omega = 0.05$. The other simulation parameters are $\zeta = 0.01$, $\kappa = 5$, and $\alpha = 1000$.

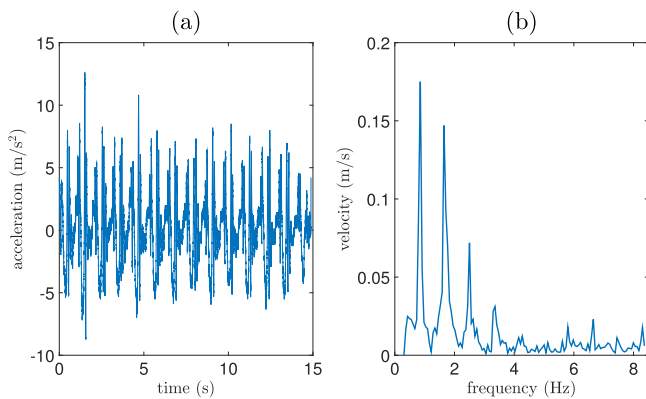


Figure 9. Non-stationary random walking excitation [31]: (a) acceleration time history recorded at the hip while walking, and (b) the velocity spectrum (Fourier transform) of the walking motion.

recorded at the hip level while walking [31]. The time history and spectral representation of the walking excitation used here are depicted in figure 9.

For simulations the experimental data are first non-dimensionalized with a scaling frequency of 500 Hz and scaling length of $20 \mu\text{m}$. Again, first the conventional bistable potential parameters (a , and x_s) are optimized for maximum harvested energy for a displacement constraint of 1.5; then the parameters of the adaptive bistable and linear harvesters are set such that they do not exceed this displacement limit. The harvested energy is computed in the same way as in the case of the harmonic excitation, with the only difference being that it is multiplied by the constant $\alpha\kappa^2$ for the sake of easier numerical comparison between different harvesters.

Figure 10(a) illustrates the displacement time history of the harvester with adaptive bistability following a BLSH logic. Energy harvested by the different harvesters is compared in figure 10(b). In addition to the optimal conventional bistable system ($x_s = 0.9$, and $a = 1.6$), two other bistable systems with detuned a parameters are simulated. According to the figure, the BLSH adaptive bistable harvester outperforms the optimal conventional bistable and the linear harvesters. It can also be seen that changes in the bistable system

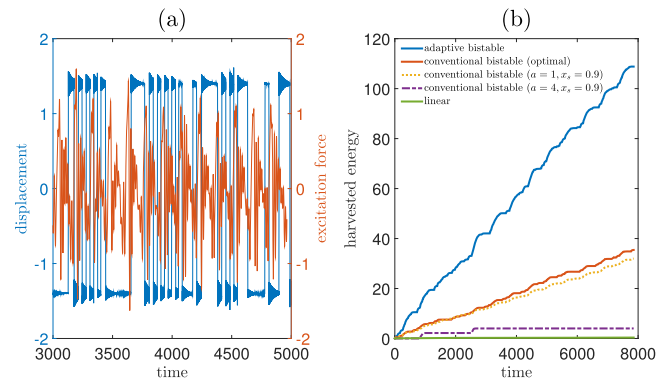


Figure 10. Energy harvesting from walking motion: (a) displacement time history of the harvester mass with adaptive bistability subjected to a displacement constraint of $|x_{\max}| < 1.5$, and (b) energy harvesting time histories of the linear, adaptive bistable, and conventional bistable harvesters. Three conventional bistable harvesters with different parameters are tested. Simulation parameters $\zeta = 0.01$, $\kappa = 5$, and $\alpha = 1000$ are used.

parameters could significantly diminish the harvester's effectiveness. Despite the differences in the governing dynamic equations and proposed harvester mechanisms, the results in figure 10 look similar to those in [22]; the reason is that both the latch-assisted mechanism in [22] and the adaptive bistable system in this study try to mimic the same BLSH logic, and given the same transduction mechanism and excitation input these two mechanisms will ideally harvest the same energy.

4. Conclusions

In this paper, the major drawbacks of linear and bistable vibration energy harvesters were pointed out and a novel non-resonant adaptive bistable harvester was proposed to overcome them. The adaptive bistable harvester follows a buy-low-sell-high strategy. In this strategy, the harvester mass is held at the lowest displacement limit ($-x_{\max}$) before the excitation force reaches its maximum, and the harvester mass is then pushed to the highest displacement limit (x_{\max}) and is held there waiting for the excitation force to reach the minimum and do the same thing in reverse. Although this strategy guarantees maximum harvested energy in an ideal harvester with no mechanical damping, it was shown by simulations that it also works pretty well with more realistic set-ups.

The paper also discussed how the adaptive bistable system could be used to enforce the BLSH strategy, and how this could be implemented in practice. It was shown that a harvester equipped with adaptive bistability following a BLSH logic significantly outperforms its linear and conventional bistable counterparts under both harmonic and experimental non-stationary random walking excitations. Also the proposed harvester does not suffer from the robustness issues that affect the linear and conventional bistable systems when the system parameters are detuned. Additionally, it was observed

that at low frequency excitations the conventional bistable system tries to mimic the BLSH strategy, which gives an insight into why the conventional bistable harvester is more effective than its linear counterpart at low frequency excitations.

References

- [1] Anton S R and Sodano H A 2007 *Smart Mater. Struct.* **16** R1
- [2] Hosseinloo A H, Vu T L and Turitsyn K 2015 arXiv:1508.04163
- [3] Hosseinloo A H, Yap F F and Chua E T 2014 *Aerosp. Sci. Technol.* **35** 29–38
- [4] Hosseinloo A H, Tan S P, Yap F F and Toh K C 2014 *Appl. Therm. Eng.* **73** 1076–86
- [5] Hosseinloo A H, Yap F F and Lim L Y 2015 *J. Vib.* **21** 468–82
- [6] Hosseinloo A H, Yap F F and Vahdati N 2013 *Int. J. Struct. Stab.* **13** 1250062
- [7] Tang L, Yang Y and Soh C K 2010 *J. Intell. Mater. Syst. Struct.* **21** 1867–97
- [8] Daqaq M F, Masana R, Erturk A and Quinn D D 2014 *Appl. Mech. Rev.* **66** 040801
- [9] Erturk A, Hoffmann J and Inman D 2009 *Appl. Phys. Lett.* **94** 254102
- [10] Mann B and Owens B 2010 *J. Sound. Vib.* **329** 1215–26
- [11] Stanton S C, McGehee C C and Mann B P 2010 *Physica D* **239** 640–53
- [12] Erturk A and Inman D 2011 *J. Sound Vib.* **330** 2339–53
- [13] Quinn D D, Triplett A L, Bergman L A and Vakakis A F 2011 *J. Vib. Acoust.* **133** 011001
- [14] Masana R and Daqaq M F 2011 *J. Sound Vib.* **330** 6036–52
- [15] Daqaq M F 2011 *J. Sound Vib.* **330** 2554–64
- [16] Cottone F, Vocca H and Gammaitoni L 2009 *Phys. Rev. Lett.* **102** 080601
- [17] Daqaq M F 2012 *Nonlin. Dynam.* **69** 1063–79
- [18] Litak G, Friswell M and Adhikari S 2010 *Appl. Phys. Lett.* **96** 214103
- [19] Halvorsen E 2013 *Phys. Rev. E* **87** 042129
- [20] Zhao S and Erturk A 2013 *Appl. Phys. Lett.* **102** 103902
- [21] Green P L, Papatheou E and Sims N D 2013 *J. Intell. Mater. Syst. Struct.* **24** 1494–505
- [22] Hosseinloo A H and Turitsyn K 2014 arXiv:1410.1429
- [23] Mitcheson P D, Green T C, Yeatman E M and Holmes A S 2004 *J. Microelectromech. Syst.* **13** 429–40
- [24] Mitcheson P D, Yeatman E M, Rao G K, Holmes A S and Green T C 2008 *Proc. IEEE* **96** 1457–86
- [25] Ramlan R, Brennan M, Mace B and Kovacic I 2010 *Nonlin. Dynam.* **59** 545–58
- [26] Heit J and Roundy S 2014 *J. Phys.: Conf. Ser.* **557** 012020
- [27] Halvorsen E, Le C, Mitcheson P and Yeatman E 2013 *J. Phys.: Conf. Ser.* **476** 012026
- [28] Ouellette S A and Todd M D 2014 *Proc. SPIE Smart Struct. Mater.* **9057** 90570Y
- [29] Tang L, Yang Y and Soh C K 2012 *J. Intell. Mater. Syst. Struct.* **23** 1433–49
- [30] Friswell M I, Ali S F, Bilgen O, Adhikari S, Lees A W and Litak G 2012 *J. Intell. Mater. Syst. Struct.* **23** 1505–21
- [31] Kluger J M 2014 Nonlinear beam-based vibration energy harvesters and load cells *Master's Thesis* Massachusetts Institute of Technology